

The Use of Stratigraphic Architecture and Rock Strength for Improved Carbonate Fractured Reservoir Modeling - Examples from Outcrop Analogs and Subsurface Reservoirs*

Chris Zahm¹ and Charles Kerans²

Search and Discovery Article #120097 (2012)

Posted December 31, 2012

*Adapted from extended abstract prepared in conjunction with poster presentation at AAPG Hedberg Conference, Fundamental Controls on Flow in Carbonates, July 8-13, 2012, Saint-Cyr Sur Mer, Provence, France, AAPG©2012

¹Bureau of Economic Geology, University of Texas at Austin, Austin, TX (chris.zahm@beg.utexas.edu)

²Department of Geological Sciences, University of Texas at Austin, Austin, TX

Abstract

Carbonate facies and the stratigraphic principles that determine their lateral and vertical distribution also define the most important heterogeneity within fractured reservoirs - how the reservoir is layered (i.e. stratal geometry and bed thickness) and how facies of differing rock strength are distributed within the volume of interest. Establishing the relationship between rock properties such as porosity, density, rock strength (e.g. unconfined compressive strength or elasticity), and facies or lithofacies can be critical for predicting how fracture intensity may change spatially within a reservoir. This study explores the relationship between the stratigraphic architecture, which controls the distribution of facies, porosity, and rock strength, and the development of fractures in outcrop analogs and in seismically-mapped faults in subsurface carbonate reservoirs.

We have established a relationship between sequence stratigraphy and mechanical stratigraphy that incorporates facies, rock properties, and bed thickness, herein referred to as vertical mechanical facies associations (VMFA). Outcrop and subsurface observations suggest nine stratal relationships that have significant influence on fracture style ([Figure 1](#)): (1) massive mound, (2) massive grainstone, (3) mixed grainstone packstone to grain-dominated packstone, (4) mixed grainstone to packstone, (5) mixed grain-dominated packstone to wackestone, (6) mixed wackestones and packstone, (7) wackestone and grain-dominated packstone to grainstone, (8) mixed shale and grain-dominated packstone to grainstone, and (9) very thin shale beds. These nine relationships become the building blocks of a mechanical stratigraphic model.

Establishing the link between the VMFA and rock properties has been done in outcrop, core and well logs. In outcrop and core, we have documented the link between facies, rock strength, and other rock properties by utilizing rebound hammers (i.e. Schmidt hammer in outcrop and micro-rebound hammer in core), which measure unconfined compressive strength of the rock ([Figure 2](#)). Outcrop analogs also provide an

excellent opportunity to establish a broader context of VMFA within important sequence stratigraphic successions, namely transgressive- and highstand-systems tracts (Zahm et al., 2010). The most important observation from outcrop is that individual beds may dictate bed-bound fracture intensity; it is the VMFA that controls the more widely-spaced but potentially highly conductive through-going fracture intensity.

Modeling

Rock cores from Aptian- and Albian-age subsurface fields in the greater Gulf of Mexico and Campos Basin have been described for carbonate fabric and lithology as well as being analyzed for rock strength. Results of this work illustrate the importance of rock fabric, especially the presence of carbonate mud on rock strength (Zahm and Enderlin, 2010). However, incorporation of core plug and well log porosity (i.e. both neutron and density porosity) illustrate the importance of total porosity on fracture development. In one subsurface study, it can be demonstrated that 85% of the fracture development within the field occurred in carbonates with less than 8% porosity (Figure 3). Furthermore, a strong empirical relationship between porosity and elasticity (e.g. dynamic Young's modulus) exists within this fractured carbonate (Figure 4). Most of the fractures within the field occurred within facies with elasticity of 50 GPa or higher (Figure 3).

The relationship between elasticity, porosity and fracture development can provide an essential link for fracture modeling, as one of the main focal points of geomodel construction is the distribution of porosity within a 3D volume of interest. We have utilized this relationship, in combination with VMFA characterization to construct a mechanical stratigraphy model for subsurface reservoirs and outcrop analogs. We believe that the mechanical facies model can be utilized in the construction of fracture models, whether they are discrete or otherwise. As a demonstration of our proposed technique, we have utilized the mechanical facies model to construct an integrated model of stratigraphy and rock properties from an outcrop analog of a carbonate fault damage zone. In this outcrop analog, we demonstrate that fracture intensity varies by both facies and by VMFA (Figure 5). We use a simple Euclidian distance to mapped fault function and vary a negative exponential slope by facies and rock strength. The VMFA aids in the control of fracture height and spacing of both bed- and VMFA-bound (i.e. through-going) fractures (Figure 6). The resultant model illustrates an improved fault damage zone model that properly reflects the stratigraphic influence on the damage zone size and shape of fractures.

Results and Conclusions

Combining the principles obtained from outcrop, core and well log, we have developed an integrated fractured carbonate reservoir model. Within the field of interest, numerous seismically-mapped faults exist within a 400-m carbonate reservoir that has mixed grain- and mud-rich dolostones and limestones. VMFA's were logged in the vertical and deviated wells within the field and a vertical proportion curve was developed that allowed for the construction of a 3D geomodel populated with mechanical facies (Figure 7). The mechanical model integrates facies, bed thickness, porosity and elasticity and is used as the architecture of the field-wide discrete fracture model (DFM). Extensional faulting is the primary mechanism responsible for fracture development within the field of interest.

Using the VMFA geomodel, we constructed an integrated fault damage zone DFM (Figure 8). Within this model, the fracture height was related to the VFMA along with fracture length as we assumed a relationship of 3:1 length-to-height ratio for grain-rich rocks and a 10:1

ratio for carbonate mud-rich facies. Fracture orientation was controlled by FMI log interpretation and seismic-processing of the post-stack data. Aperture was assumed to be a power law distribution and proportional to fracture length. The resultant model was constructed using Fracman© ([Figure 9](#)) and upscaled to an equivalent permeability which was used for field-wide history match and validation ([Figure 10](#)). Pressure match to both individual well test and field-wide production validates the concept of a dispersed fault-related fracture zone model, further underscoring the importance of integration of stratigraphy and fractures within dual-permeability reservoirs.

References

- Zahm, C., L. Zahm, and J.A., Bellian, 2010, Integrated fracture prediction using sequence stratigraphy within a carbonate fault damage zone, Texas, USA: *Journal of Structural Geology*, v. 32, p. 1363-1374.
- Zahm, C.K., and M. Enderlin, 2010, Characterization of rock strength in Cretaceous strata along the Stuart City Trend, Texas: *Gulf Coast Association of Geological Societies Transactions*, v. 60, p. 693-702.

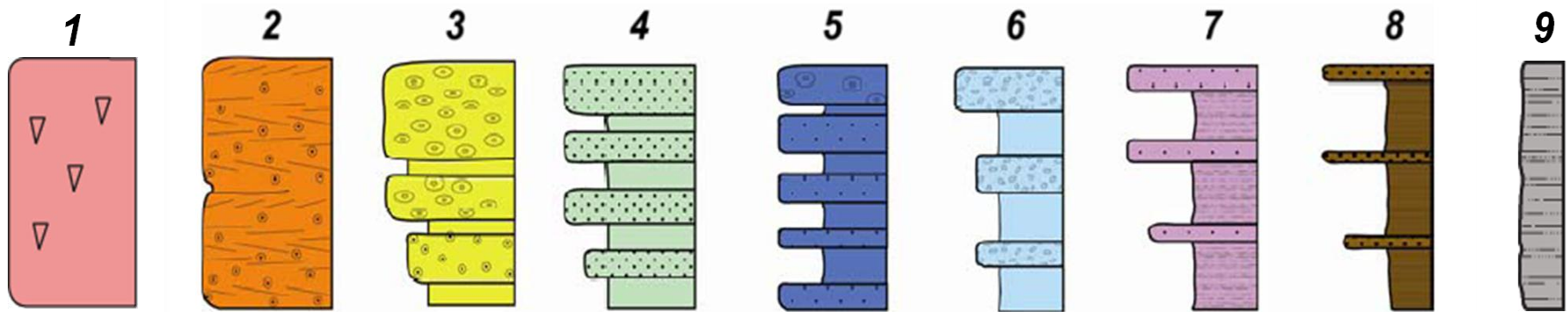


Figure 1. Nine fundamental stratal relationships that comprise a vertical mechanical facies association (VMFA) including: (1) massive mound, (2) massive grainstone, (3) mixed grainstone packstone to grain-dominated packstone, (4) mixed grainstone to packstone, (5) mixed grain-dominated packstone to wackestone, (6) mixed wackestones and packstone, (7) wackestone and grain-dominated packstone to grainstone, (8) mixed shale and grain-dominated packstone to grainstone, and (9) very thin shale beds.

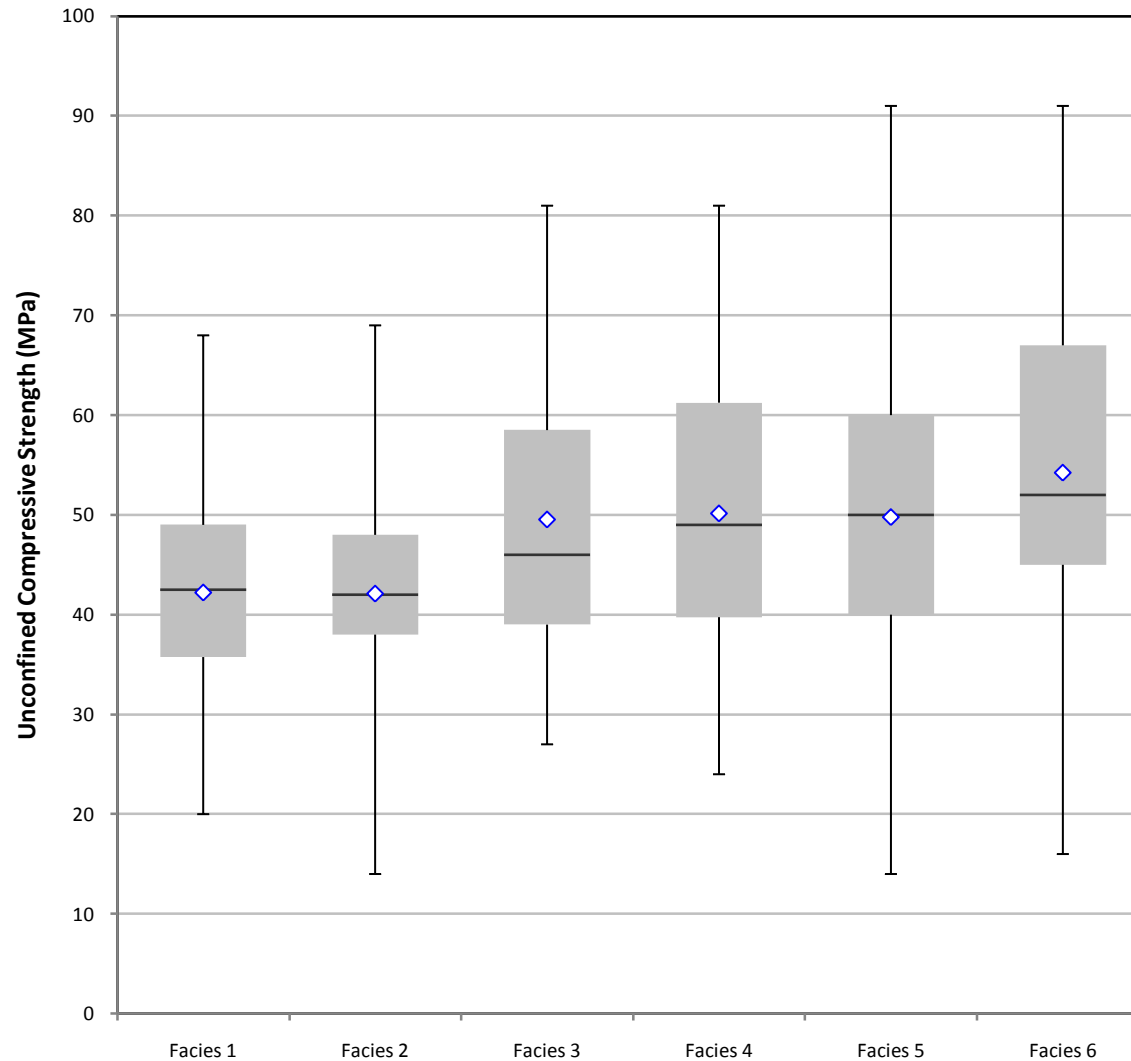


Figure 2. Box-and-whisker plot of unconfined compressive strength (MPa) measured in cores using a micro-rebound hammer where Facies 1 is an oolitic grainstone; Facies 2 is an oncolitic rudstone; Facies 3 is a grain-dominated packstone; Facies 4 is a mixed skeletal grain-dominated packstone; Facies 5 is a burrowed, peloidal wackestone; and Facies 6 is an argillaceous mudstone. The box represents the lower and upper quartile of the data, whereas the whiskers are the full minimum and maximum measured data values.

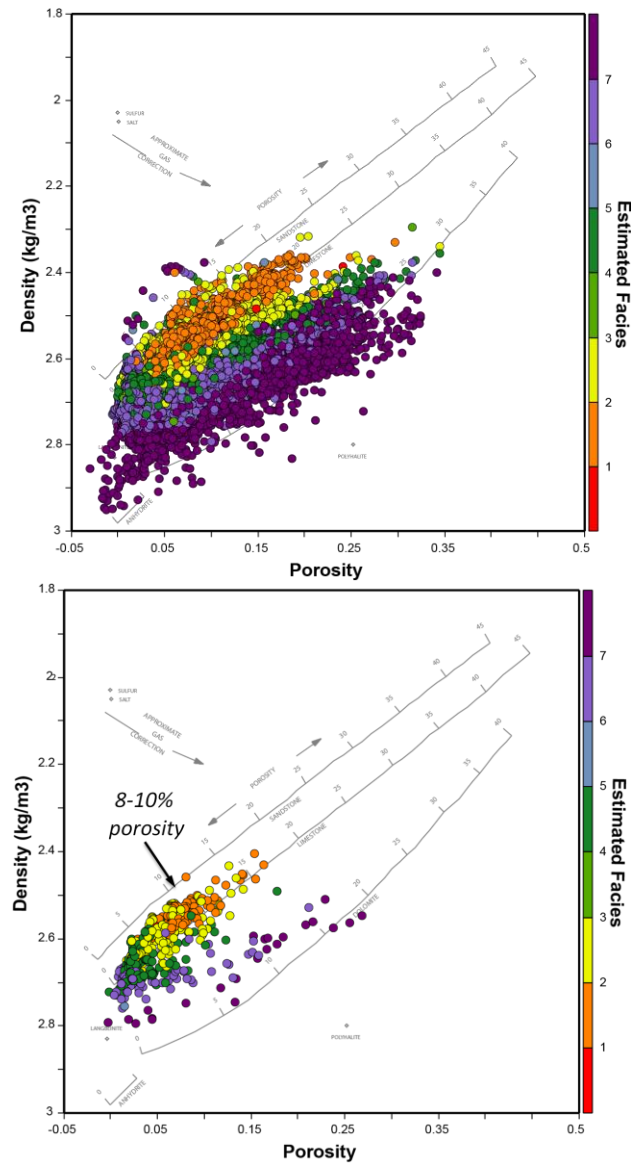


Figure 3. Density-porosity cross plot from well logs colored by facies. Plot A represents the entire reservoir interval, whereas Plot B is from the same interval, but only where open fractures are present. Note that a large majority of the fractures within this reservoir occur in rocks with less than 8% porosity. In these two figures the dark purple points are dolostones.

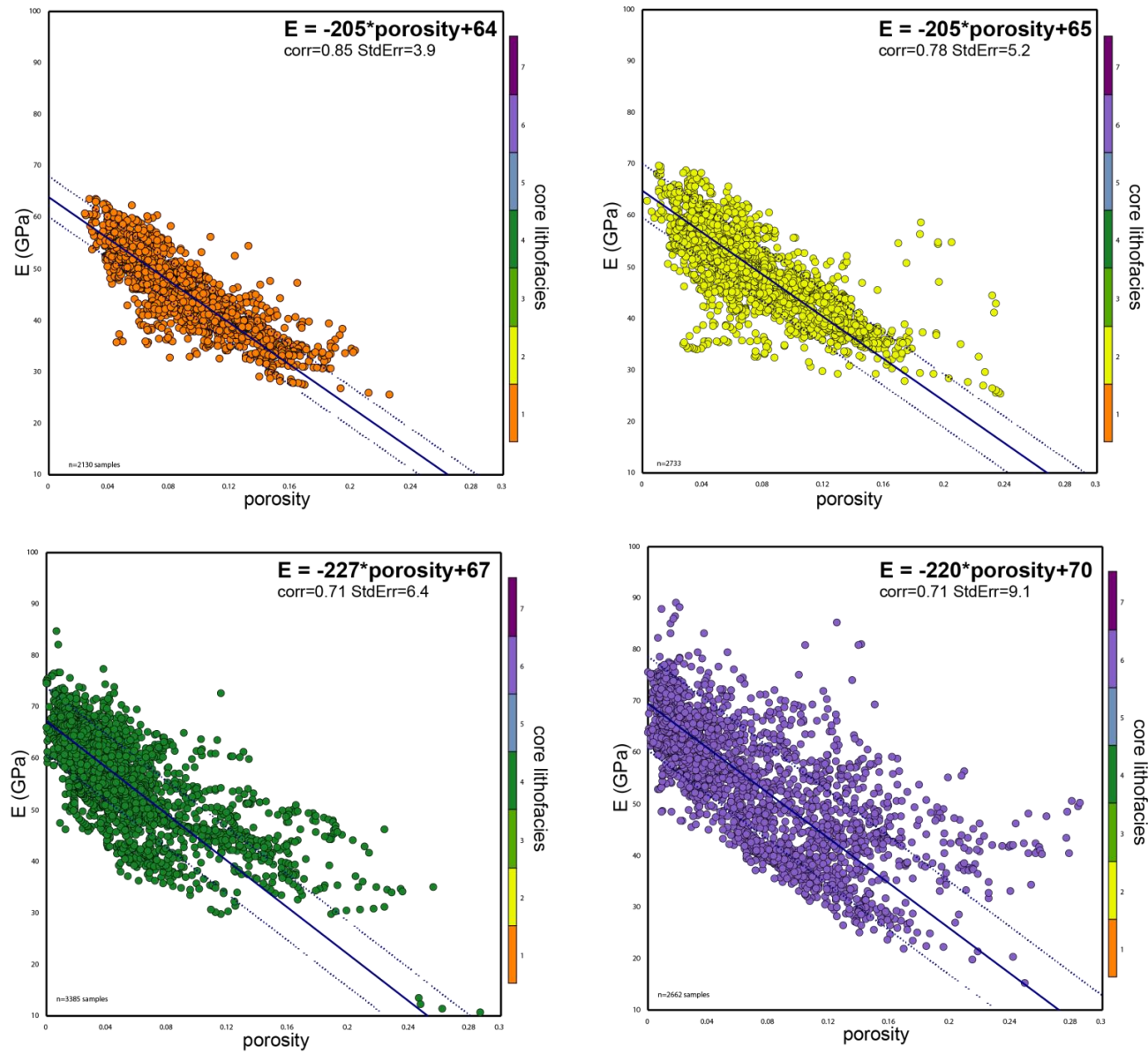


Figure 4. Cross plot of log-calculated elasticity versus neutron porosity. The four plots are all limestones, but they are separated by rock fabric facies: (A) oolitic grainstones; (B) oncolitic rudstones; (C) mud-dominated grainstones; and (D) packstones to wackestones.

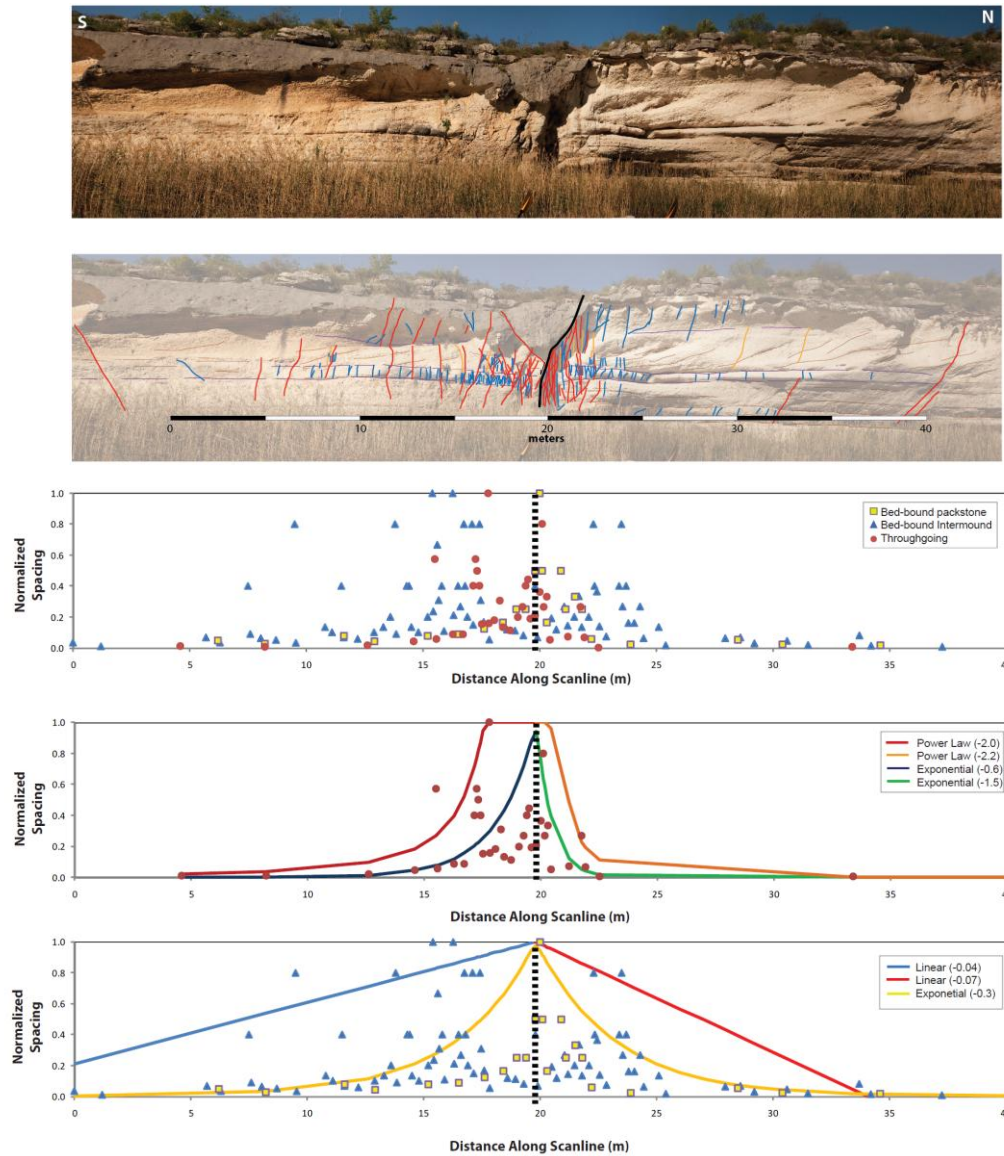


Figure 5. Fault damage zone characterization by facies for both bed-bound and throughgoing fractures. Top photo is of a small fault in outcrop. The upper portion of the cliff is a grain-dominated packstone, the middle portion is a skeletal grainstone between biostromal mounds. This is underlain by a thin, wackestone bed with high fracture intensity near to the fault. The top plot is the normalized spacing as measured away from the fault for the three fracture populations: (1) mud-rich facies (blue); (2) grainstone (yellow); and throughgoing (red). The bottom two plots show the impact of fitting power-law, negative exponent and linear decays away from the mapped fault.

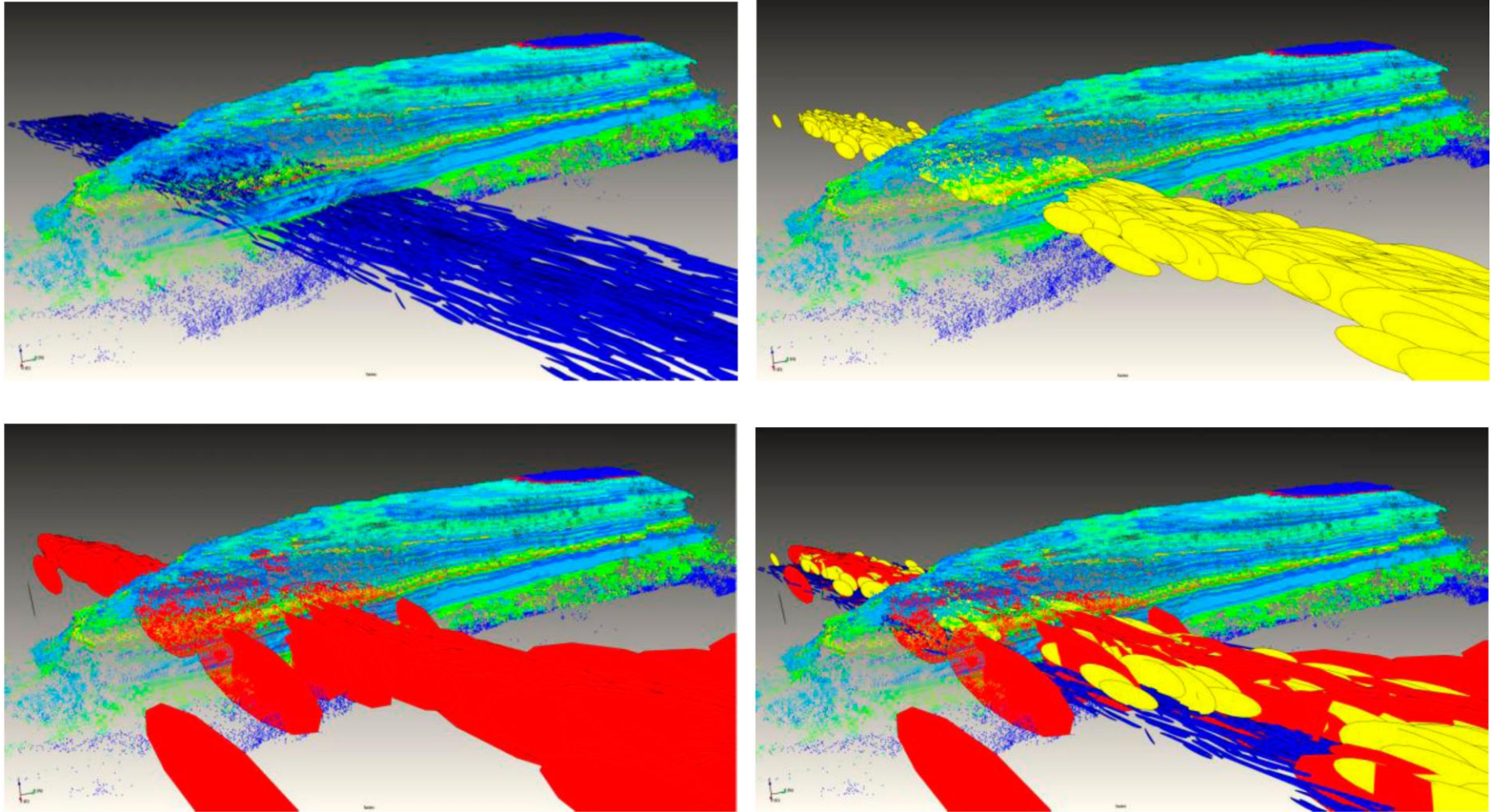


Figure 6. Integrated fault-related fracture damage zone where different facies contain different fracture spacing and size distributions. (A) Mud-rich facies with small fracture heights and high intensity (low spacing); (B) Grain-rich facies with larger fracture heights and lower intensity; (C) throughgoing fractures which span the entire fourth-order cycle; (D) composite of three fracture populations within an integrated stratigraphy and fault-related fracture model. Note that the background of the image is a lidar-scanned point cloud of the nose of two adjoining canyons. The colors on the point cloud represent the facies mapped on the outcrop scan.

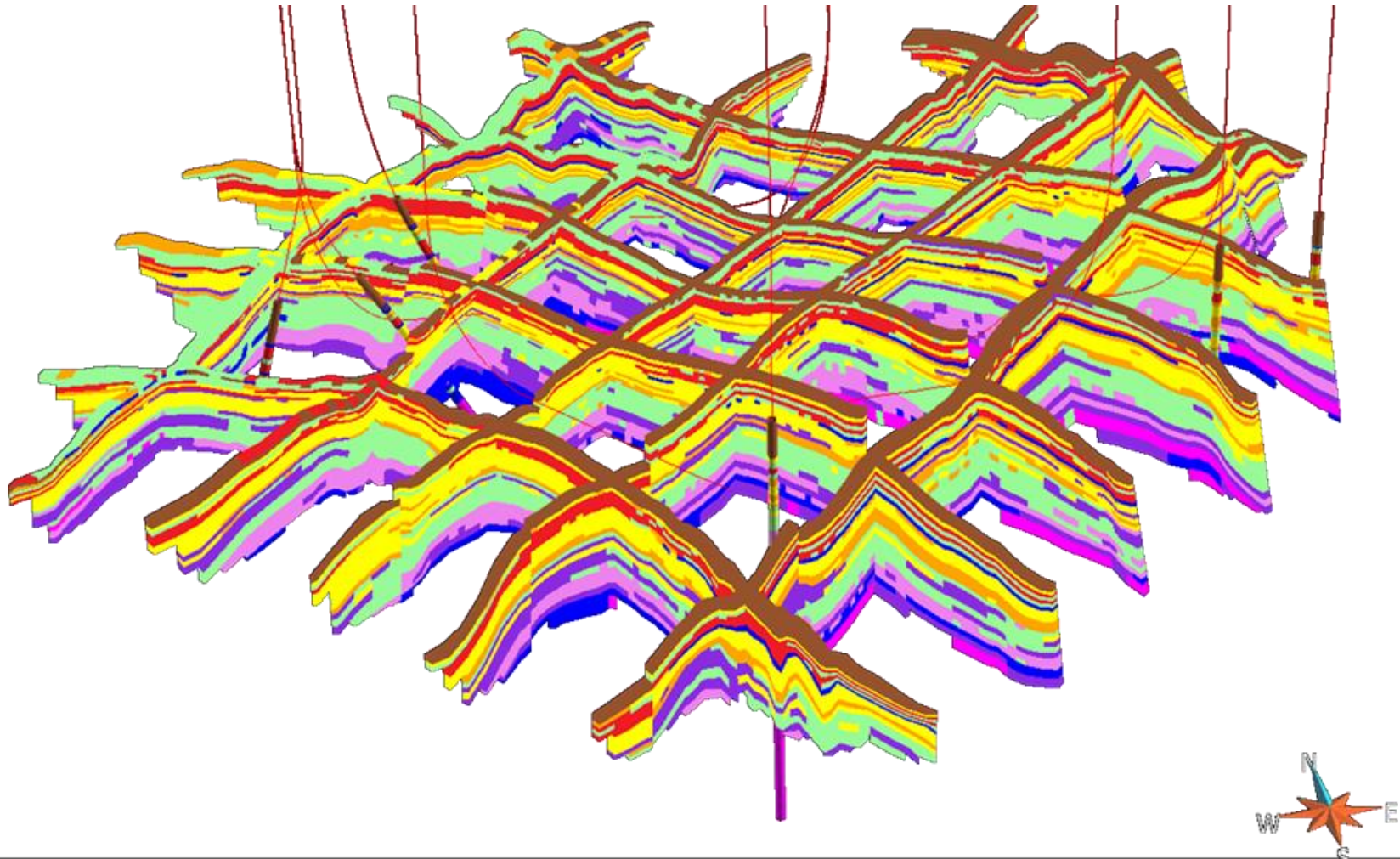


Figure 7. 3D geomodel with distributed VMFA properties based on six vertical or deviated wells within the field of interest. Vertical proportion curves were generated from the well logs and the properties were distributed using sequential-gaussian simulation (SGS).

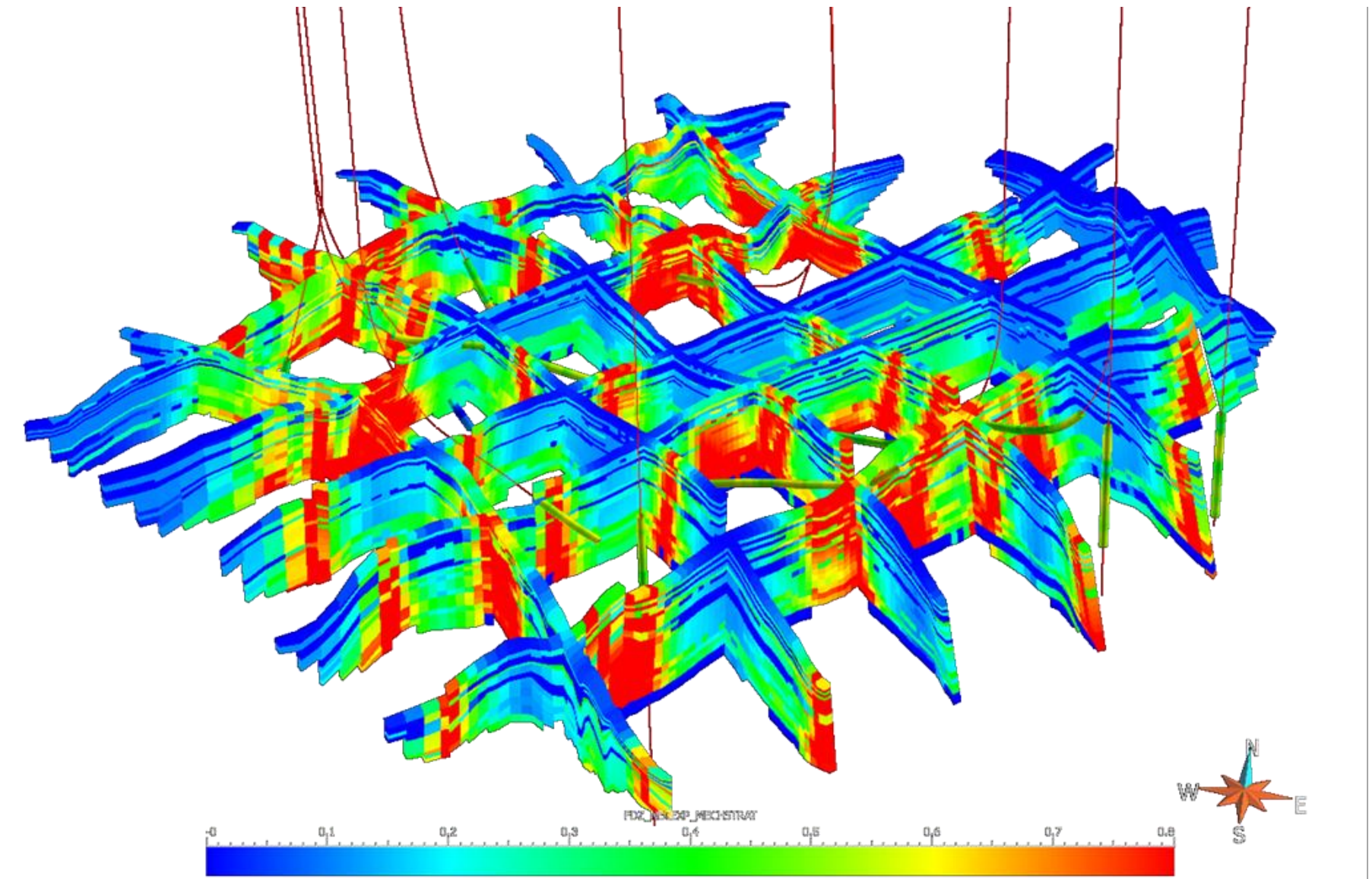


Figure 8. Integrated fault-damage zone model which uses different negative exponent slopes based on rock properties. Warm colors represent areas immediately adjacent to seismically-mapped faults, whereas cooler colors represent areas that have less fractures away from the mapped faults. The VMFA model is integrated with the seismic faults and different slopes are applied based on rock strength properties.

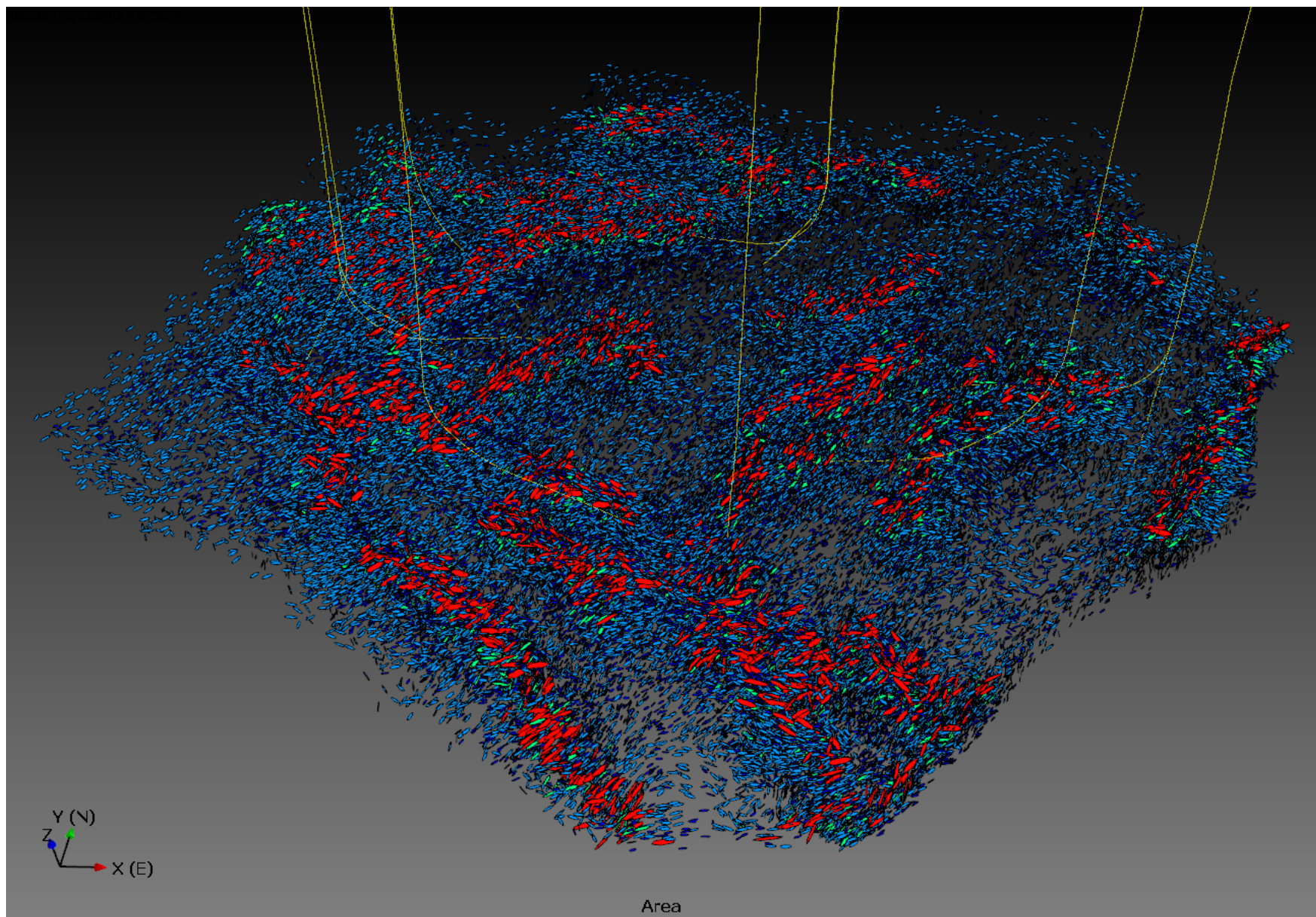


Figure 9. Discrete fracture network for the constructed integrated model. Fracture colors vary from red for larger fractures (typically found within thick grainstones near the top of the reservoir), whereas blue fractures are smaller in size and are more common to thin-bedded VMFA zones.

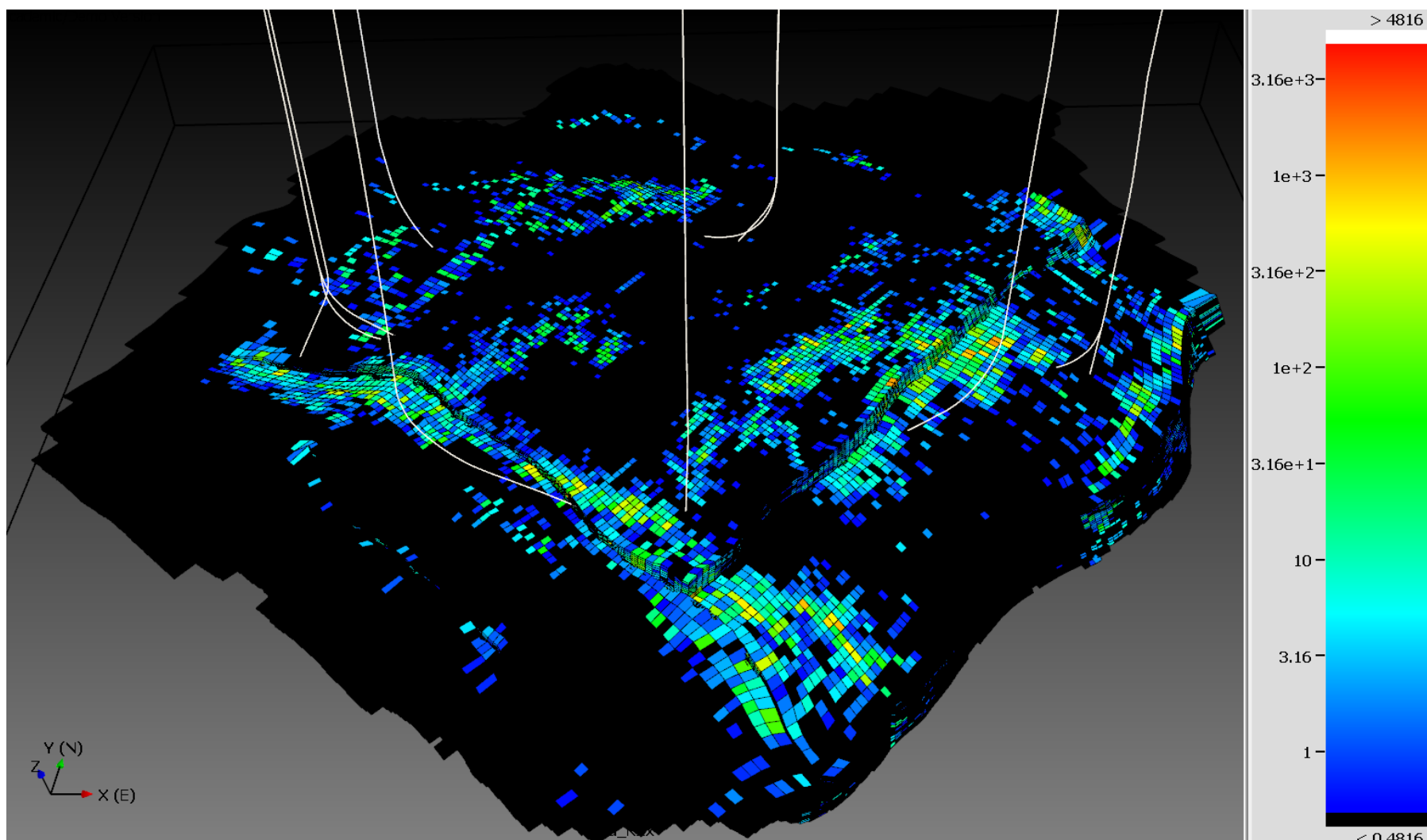


Figure 10. Upscaled equivalent fracture permeability (K_{xy}) from field of interest based on the VMFA geomodel and fault damage zones of seismically-mapped faults. Permeability scale is in millidarcies.